# A Measurement of the Air Fluorescence Yield

F.Kakimoto[a], E.C.Loh[b], M.Nagano[c]

H.Okuno[d], M.Teshima[c], S.Ueno[a]

[a] *Department of Physics, Tokyo Institute of Technology, Meguroku, Tokyo 152, Japan*

[b] *High Energy Astrophysics Institute, Department of Physics,*

*University of Utah, Salt Lake City, Utah, UA84112 USA*

[c] *Institute for Cosmic Ray Research, University of Tokyo, Tanashi, Tokyo 188, Japan*

[d] *Institute for Nuclear Study, University of Tokyo, Tanashi, Tokyo 188, Japan*

**Abstract**

We measured the air fluorescence yield as a function of pressure with electrons between 1.4 MeV and 1000 MeV by means of a $^{90}$Sr $\beta$ source and an electron beam. Results indicate that the fluorescence yield is proportional to electron energy loss from 1.4 MeV to 1000 MeV. The $\frac{dE}{dx}$ relativistic rise in air is detected. We describe the pressure temperature dependency of air fluorescence by a formula derived from simple kinetic theory. With the aid of the 1966 US Mid-latitude Standard Atmospheric Model, we calculate the altitude dependence of fluorescence yield of an 80 MeV electron which demonstrates how this measurement could improve the longitudinal particle density profile determination of extensive air showers (EAS) observed by detectors such as the High Resolution Fly's Eye and the Telescope Array.

# 1 Introduction

Air fluorescence along a track of a cosmic ray-induced particle cascade, detected and measured by the Fly's Eye Detector [1], was used for determining the energy, the longitudinal shower profile and the direction of the incident cosmic ray. This fluorescent light, emitted by molecular nitrogen excited by the charged particles in the EAS, is proportional to the number of particles in the cascade, and depends weakly on the pressure and temperature of the atmosphere.

Air fluorescence yield (which we define as the number of photons produced by a charged particle per meter of travel) in the near UV and in the visible region is the strongest between 300 and 400 nm [2]. With the exception of the 391.4 nm line, which is the $N_2^+$ first negative system, air fluorescence in this wavelength region is due to the $N_2$ second positive system [2]. The air fluorescence yield is, however, much lower than the fluorescence yield of pure nitrogen. The low yield of air is attributed to the presence of oxygen molecules, which by their many low lying energy states lower the fluorescence yield by collision de-excitation [3]. Results of early measurements of the air fluorescence yield differed by as much as 30$\sim$40%. The Fly's Eye quoted this difference as the systematic uncertainty which is the dominant systematic uncertainty in the Fly's Eye's measurement of the primary cosmic ray differential energy spectrum [4].

Two new detectors based on the fluorescence technique, the High Resolution Fly's Eye Detector (HiRes) [5] currently under construction and the Telescope Array [6] currently under development, possess better optics and are intrinsically capable of measuring shower profiles with much greater precision than the Fly's Eye Detector. A more precise measurement of the air-fluorescence efficiency is required in order to exploit the full designed capabilities of these new detectors.

An early measurement of air fluorescence yield by Davidson *et al.* [2] was carried out at a pressure of 600 mmHg with 50 keV electrons stopping in air. Bunner measured the air fluorescence [3] with 4 MeV $\alpha$ particles stopping in air. Since particles in extensive air showers are dominated by electrons with energy above tens of MeV, we measured the air fluorescence yield with electrons at 1.4 MeV, 300 MeV, 650 MeV, and 1000 MeV bracketing the energy region of interest.

# 2 Experiment

We chose a photon counting and thin target technique to measure the fluorescence yield of air with electrons at various air pressure.

A cylindrical tank, shown in Fig.1, was built for this experiment. Five quartz-covered ports, providing viewing of the interior of the tank, were placed on the wall of the cylinder. A shutter was built in front of each port inside the tank, providing obscuration of the photomultiplier tube (PMT) for background measurements. Four Hamamatsu photon counting PMT's, H1161PX, selected for low noise were mounted on the ports to observe the fluorescent light.

Three narrow band filters, whose transmission coefficients are shown in Fig. 2, were used for measuring the intensity of 337.1, 357.7, and 391.4 nm bands. A broad band filter (Fig. 2), used in the HiRes, was used to measure the overall yield between 300 and 400 nm.

For the 1.4 MeV measurement, we used a 1 mCi $^{90}$Sr source. For this measurement a special holder was made to secure the source inside the tank. A small scintillation counter was placed 95 mm from the source to detect the electrons emitted from the source. The coincidence between the photon PMT's and the scintillation counter was used to generate a gate for a multiple channel ADC and a start gate for a TDC. The electron rate was about $1.4\times10^4$/s.

Electrons extracted from the Electron Synchrotron of the Institute for Nuclear Study (INS, University of Tokyo) were used for the 300, 650, and 1000 MeV measurements. The experimental layout is shown in Fig. 3. We centered the extracted beam (whose diameter was 5 mm) on the entrance and exit windows of the tank with the aid of Polaroid film. A thick (about 2.4 radiation lengths) ionization chamber was used as a beam monitor. Two counters, C and D, were placed behind the thick ionization chamber. A pair of counters, A and B, was installed behind the tank and in front of the thick ionization chamber. During measurements of the fluorescence yield, the beam rates were about $6\times10^5$/s sufficiently high so that counters A and B could not be used to monitor the beam intensity. The number of electrons going through the tank were calculated from the charge in the ionization chamber and also from the number of particles that registered in counters C and D. We calibrated the ionization chamber by counting particles going through counters A, B, C, and D and measured the charge through the thick ionization chamber (The beam was varied from $10^3$/s to $10^6$/s by tuning the linac injector). In this way, we obtained the calibration constant of the ionization chamber, which is the charge per incident beam particle, and at the same time obtained the calibration constant for C and D, which is particles through C and D per incident beam particle. During calibration, the rates for C and D were greatly reduced by means of absorbers placed between the ionization chamber and counters C and D so that the rates in the counters were at a usable level at the highest intensity used.

To achieve the best signal to noise ratio, we covered the entire tank with a lead shield 10 cm thick and moved the front window farther from the PMT's by a 500 mm long tube. A vacuum pipe was placed between the tank and the ionization chamber to reduce background and multiple scattering of the beam.

For runs with the extracted beam, an internal pipe was installed which limited the visible part of the electron path to 10 cm and obscured the Čerenkov light emitted by the beam electrons. Scattered Čerenkov light was calculated to be negligible.

Dry air with dew point of -50°C was used throughout the experiment. For purposes of obtaining counting efficiency and setting biases, we used 99.998% pure nitrogen whose yield was about a factor of 5.6 higher than that of air.

# 3 Results

## 3.1 1.4 MeV Measurement

A typical single photon pulse height spectrum and a distribution of photon relative to the electron time intervals are shown in Fig. 4 and Fig. 5.

We obtained, for a fixed number of electrons registered by the scintillation counter, the coincidence counts between the electron counter and the four photon PMT's. We first separated

the background from the signal. From the TDC distribution, we identified the signal region, a region around the TDC peak. We then used the remaining portion of the TDC distribution to calculate the background in the signal region. Signal was the counts in the region after the background was subtracted. Using the ratio of signal count per incident electron, the visible beam length, the quantum efficiency, the collection efficiency, the filter transmission, the quartz window transmission, and the solid angle of the PMT, we calculated the yields (photons emitted by an electron per meter) from data obtained with the narrow band filters. A computer readout dead time correction, about 1.5%, was applied.

In order to obtain the fluorescence yield between 300 and 400 nm, we needed the spectrum which was calculated from the data collected with the HiRes filter. The method by which we obtained the spectrum is outlined below: Using the Davidson fluorescence efficiency measurement between 300 and 400 nm as the relative spectrum, we inserted the yields of the 3 bands. We obtained the spectrum by adjusting the remaining spectrum normalization until we replicated the HiRes filter experimental results. The three bands accounted for about 70% of the fluorescence photons in this wavelength region. Knowing the spectrum, we used the method mentioned above to obtain the yield between 300 and 400 nm.

The fluorescence yields by 1.4 MeV electrons for the 337, 357, and 391 nm bands and for the wavelength between 300 and 400 nm as a function of pressure are shown in Fig. 6. Uncertainties shown are statistical.

### 3.2 300, 650, and 1000 MeV Measurements

Because the electron beam extracted from the Synchrotron has approximately 5∼10% duty cycle, it was not possible to perform coincidence measurement as was used in the $^{90}$Sr case. For measurements using the electron beam, we counted the single rates of the PMT's and the beam monitor readings gated only by the beam spill gate. Subsequently, the PMT's were covered by the shutters in front of them and counts were obtained for the same quantity of monitor counts. In this way, we subtracted out the background counts, which was of the order of 20%, and obtained the number of counts due to air fluorescence light along a 10 cm particle trajectory. We also examined randomly the pulse height of the photon PMT's by an ADC unit triggered by the single rate of the PMT's gated on during the beam spill. The shapes of the pulse height spectrum obtained were exactly the same as those obtained with the source by the coincidence method. This confirms that we were detecting single photon events resulting from the beam. For each beam energy we obtained the counts attributed to air fluorescence per unit thick ionization chamber charge, as well as the number of counts per C and D coincidence. Knowing the calibration constants of the beam monitors, we calculated the fluorescence yield using the method outlined in the previous section.

The fluorescence yield at 760 mmHg as a function of incident electron energy is shown in Fig. 7. On the same plot we show the electron $\frac{dE}{dx}$ whose scale is displayed on the right hand side. A typical fluorescence yield as a function of pressure with 1000 MeV electrons is shown in Fig. 8 which is similar to those obtained with 1.4 MeV electrons. All uncertainties shown include statistics, deadtime, multiple counts in a single rf bucket, and calibration uncertainties.

### 3.3 PMT Calibration

Not shown in both the 1.4 MeV results and the beam electron results are the systematic errors due to PMT calibration: quantum efficiency (QE) and collection efficiency which were provided by the manufacturer, Hamamatsu Photonics. The collection efficiency is defined by Hamamatsu as the counts at the anode divided by the number of photons impinging on a 3 mm diameter area (which was used in this experiment) centered on the cathode. The factory collection efficiency measurement was done by counting a known intensity photon beam at a PMT gain setting of $5\times10^6$ and with a discriminator setting at 1/3 of the single photon peak. Quantum efficiency of one of the photomultipliers was checked at 351 and 365 nm at the University of Utah against a photodiode calibrated by the National Institute of Standards and Technology (NIST). Agreement between the factory quantum efficiency and that measured at the University of Utah [7] was obtained at the 8% level (difference between the two QE measurements divided by the average of two measurements is 8%). We used the two measurements to establish the QE systematic error. Factory QE was used for analysis.

Since we used a higher gain setting, $2\times10^7$, and a lower discriminator threshold, 1/10 of the observed single photon peak, we evaluated the collection efficiency for this experiment. Fitting our observed single photon spectrum to a first dynode and second dynode gain model with our gain and bias settings, we obtained a collection efficiency of 90% with a 5% uncertainty. This model also predicted the collection efficiency observed by the factory. The total systematic uncertainty due to the PMT calibration uncertainties is taken to be the above two errors added in quadrature which is 10%.

## 4 Discussion

From Fig. 7, we conclude that the fluorescence yield (in photons/meter/electron) of air between 300 and 400 nm is proportional to the electron $\frac{dE}{dx}$. Based on kinetic theory arguments, Bunner [3] pointed out that the fluorescence yield of a band is proportional to a simple formula, $yield \sim \frac{\rho}{1+\rho B\sqrt{t}}$, where $B$ is a constant, $t$ is the temperature, and $\rho$ is the density. The denominator takes into account the collision de-excitation of the nitrogen molecule. The collision de-excitation process depends on the velocity as well as on the collision cross sections. Hence the denominator has a factor containing the density and the square root of the temperature on which the velocities of the molecules depend. From the pressure dependency of the three major bands, we note that the yields of the 337 and the 357 nm bands have the same pressure dependency and the 391 nm band yield does not show much pressure dependency from atmospheric pressure all the way down to 40 mmHg. Since we have two sets of pressure dependencies, we fitted our data to the following equation with two terms :

$$yield = \frac{(\frac{dE}{dx})}{(\frac{dE}{dx})_{1.4MeV}}\rho\left\{\frac{A_1}{1+\rho B_1\sqrt{t}} + \frac{A_2}{1+\rho B_2\sqrt{t}}\right\} \quad (1)$$

where $\frac{dE}{dx}$ is the electron energy loss, $\rho$ in kg m$^{-3}$, $t$ in degrees kelvin(K), and $(\frac{dE}{dx})_{1.4MeV}$ is the $\frac{dE}{dx}$ evaluated at 1.4 MeV. Electron $\frac{dE}{dx}$ is calculated by a program supplied to us by D. Groom of the Particle Data Group at Berkeley [8] [9]. The yield between 300 nm and 400 nm is expressed

in units of photons per meter per electron.

Constants $A_1, A_2, B_1$ and $B_2$ are shown in Table 1. The relativistic rise as well as the density effect as observed is taken into account by the $\frac{dE}{dx}$ formula.

*Table 1. Constants $A_1, A_2, B_1$ and $B_2$ used in the equation (1).*

| | | | |
|---|---|---|---|
| $A_1$ | $89.0 \pm 1.7$ m$^2$ kg$^{-1}$ | $B_1$ | $1.85 \pm 0.04$ m$^3$ kg$^{-1}$ K$^{-1/2}$ |
| $A_2$ | $55.0 \pm 2.2$ m$^2$ kg$^{-1}$ | $B_2$ | $6.50 \pm 0.33$ m$^3$ kg$^{-1}$ K$^{-1/2}$ |

For comparison with Davidson *et al.* and Bunner, we calculate the fluorescence efficiency, defined as the radiated energy divided by the energy loss in the observed medium, for the three lines. Table 2 shows the results obtained by the three experiments.

*Table 2. Comparison of fluorescence efficiencies.*

| | | This Experiment | D&O [2] | Bunner [3] |
|---|---|---|---|---|
| | beam | 1.4 MeV electron | 50 keV electron | 4 MeV $\alpha$ particle |
| | pressure | 600 mmHg | 600 mmHg | 760 mmHg |
| wavelength | 337 nm | $2.1\times10^{-5}$ | $2.1\times10^{-5}$ | $1.5\times10^{-5}$ |
| | 357 nm | $2.2\times10^{-5}$ | $1.5\times10^{-5}$ | $1.2\times10^{-5}$ |
| | 391 nm | $0.84\times10^{-5}$ | $0.70\times10^{-5}$ | $0.43\times10^{-5}$ |

Davidson *et al.* quoted an error of 15% which is due to PMT calibration and beam intensity calibration and variation. Our systematic error is 10% and our statistical error is about 3%.

It should be noted that these experiments were carried out under different conditions. Bunner used 4 MeV $\alpha$ particles stopping in air, and Davidson *et al.* used 50 keV electrons stopping in air. Both of them analyzed the emission with a scanning monochrometer. For our measurement, we used fixed filters which accepted some contributions from the small side bands. While our method gives accurate overall yield between the 300 and 400 nm region, it does affect direct comparison of those obtained with monochrometers where slit widths played an important role. Nevertheless, when systematic errors are taken into account, our results agree well with those of Davidson *et al.*.

In passing, it is interesting to note that Davidson *et al.* also measured the pure nitrogen fluorescence efficiency. They obtained a nitrogen to air ratio close to 20 for 50 keV stopping electrons, while we obtain a ratio close to 5.6 in the same wavelength region. At this moment, the difference is not understood.

Using our yield between 300 and 400 nm and the 1966 Summer and Winter US Standard Atmospheric Models, we calculated the fluorescence yield of an 80 MeV electron (critical energy) as a function of altitude as shown in Fig. 9. From the surface up to the tropopause, the temperature of the atmosphere decreases about 6 degrees per kilometer. This causes the fluorescence yield to increase slightly. After reaching the tropopause, the temperature of the atmosphere becomes almost constant but the density continues to decrease, which results in the decreasing fluorescence yield. Notice also that the variation of the yield at the surface is due to temperature difference and that the tropopause height moves as the season changes. This variation of the fluorescence yield needs to be taken into account for accurate cosmic cascade energy and shower profile determination.

## 5 Conclusion

Our experiment made the first observation of air fluorescence as a function of pressure (40∼760 mmHg) using high energy electrons from 1.4 to 1000 MeV. Results indicate that the fluorescence yield is proportional to the electron $\frac{dE}{dx}$ in this energy region as shown in Fig. 7. The electron $\frac{dE}{dx}$ rise in air is observed. Air fluorescence yield, in photons per meter per electron, between 300 and 400 nm as a function of the temperature and density of air is expressed in equation (1). The results are in good agreement with Davidson *et al.* Our measurements will improve the determination of the longitudinal EAS profiles obtained with the new detectors which would result in more accurate energy measurements of cosmic rays in the highest energy region.

**Acknowledgement**

We would like to thank the staff of the Electron Synchrotron group of the Institute for Nuclear Study, University of Tokyo, for operating the synchrotron and the electron beam. Thanks also go to the staff of the INS Machine Shop for their help in designing and building the tank used in this experiment. We would also like to thank Don Groom of the LBL Particle Data Group for supplying us with the $\frac{dE}{dx}$ program as well as lending us some of the electronics. One of us (Loh) would like to express his appreciation to the Institute for Cosmic Ray Research of the University of Tokyo for their generous support of his stay in Tokyo during the data phase of this experiment. This work is supported in part by the Grant-in-Aid for Scientific Research No.06402006 from the Japanese Ministry of Education, Science and Culture and in part by a grant, INT 9217328, from the National Science Foundation of the USA.

## References

[1] R.M.Baltrusaitus *et al.*, Nucl. Instr. & Methods, **A240** (1985) 410.

[2] G.Davidson and R.O'Neil, J. Chem. Phys. **41** (1964) 3946.

[3] A.N.Bunner, PhD. Thesis, Cornell University, Ithaca, N.Y. (1964).

[4] D.J. Bird *et al.*, Ap. J. **424** (1995) 497.

[5] S.C.Corbato *et al.*, Nucl. Phys. B (Proc. Suppl.) **28B** (1992) 36.

[6] M.Teshima, Nucl. Phys. B (Proc. Suppl.) **28B** (1992) 169.

[7] D.J. Bird *et al.*, Nucl. Inst. & Meth. **A349** (1994) 592.

[8] S.M. Seltzer and M.J. Berger, Int. J. Appl. Radiat. Isot., **33** (1982) 1189.

[9] R.M.Sternheimer, M.J.Berger, and S.M.Seltzer, Atomic Data and Nuclear Data Tables **30** (1984) 261.

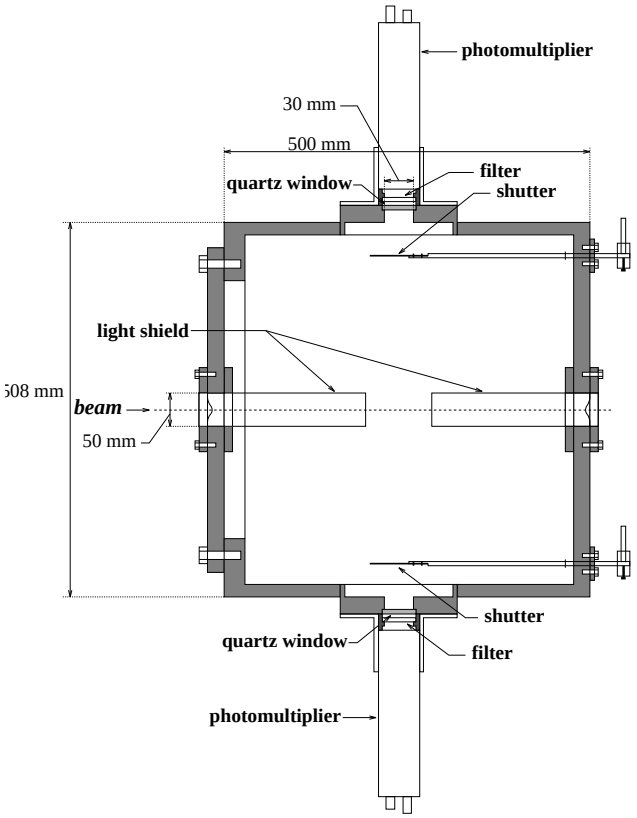


Figure 1: *Schematic drawing of the tank(top view). Four PMT's were mounted on the windows for viewing the fluorescent light. Optical filters were mounted between the photomultiplier tubes and the quartz windows.*

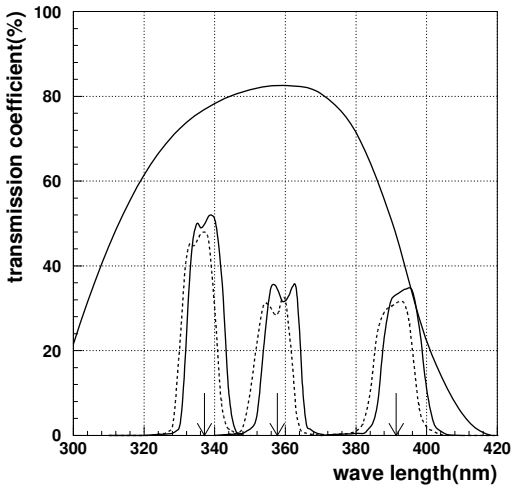


Figure 2: *Transmission coefficients of three narrow band filters and a broad band filter are shown as a function of wavelength. Two transmission curves for each narrow band filter are shown: solid line curves are for normal incidence light and dotted lines are for light with an incident angle of 10°. Three arrows indicate the position of the three lines, 337.1, 357.7 and 391.4nm.*

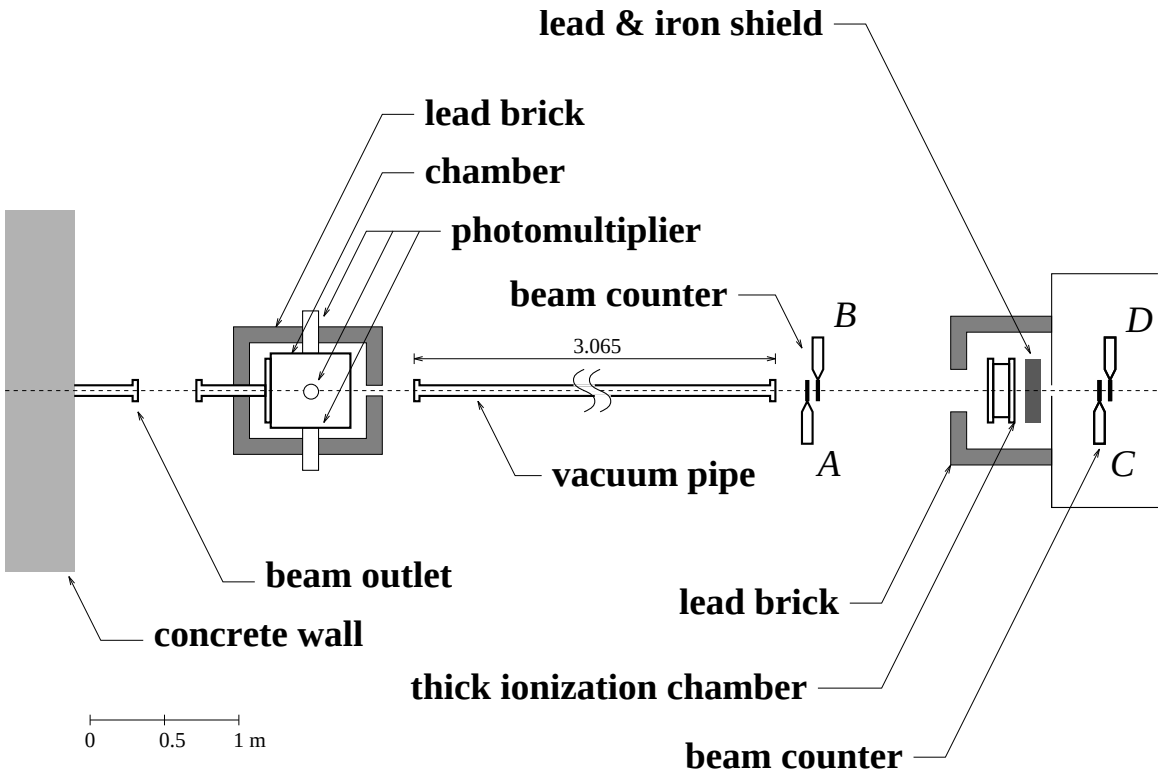


Figure 3: *Schematic layout of the experiment using the extracted electron beam from the INS Electron Synchrotron.*

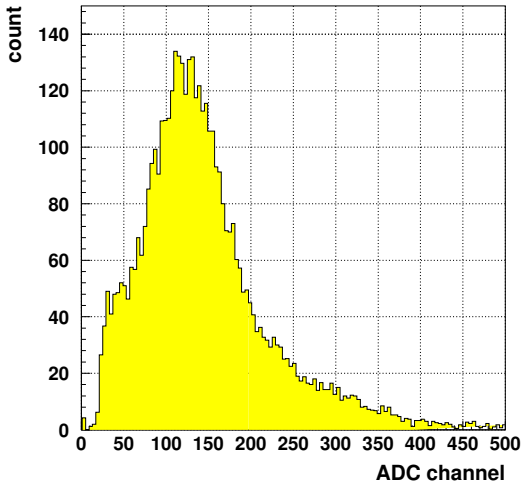


Figure 4: *A typical single photon pulse height spectrum. This spectrum was obtained with the HiRes filter at a pressure of 760 mmHg.*

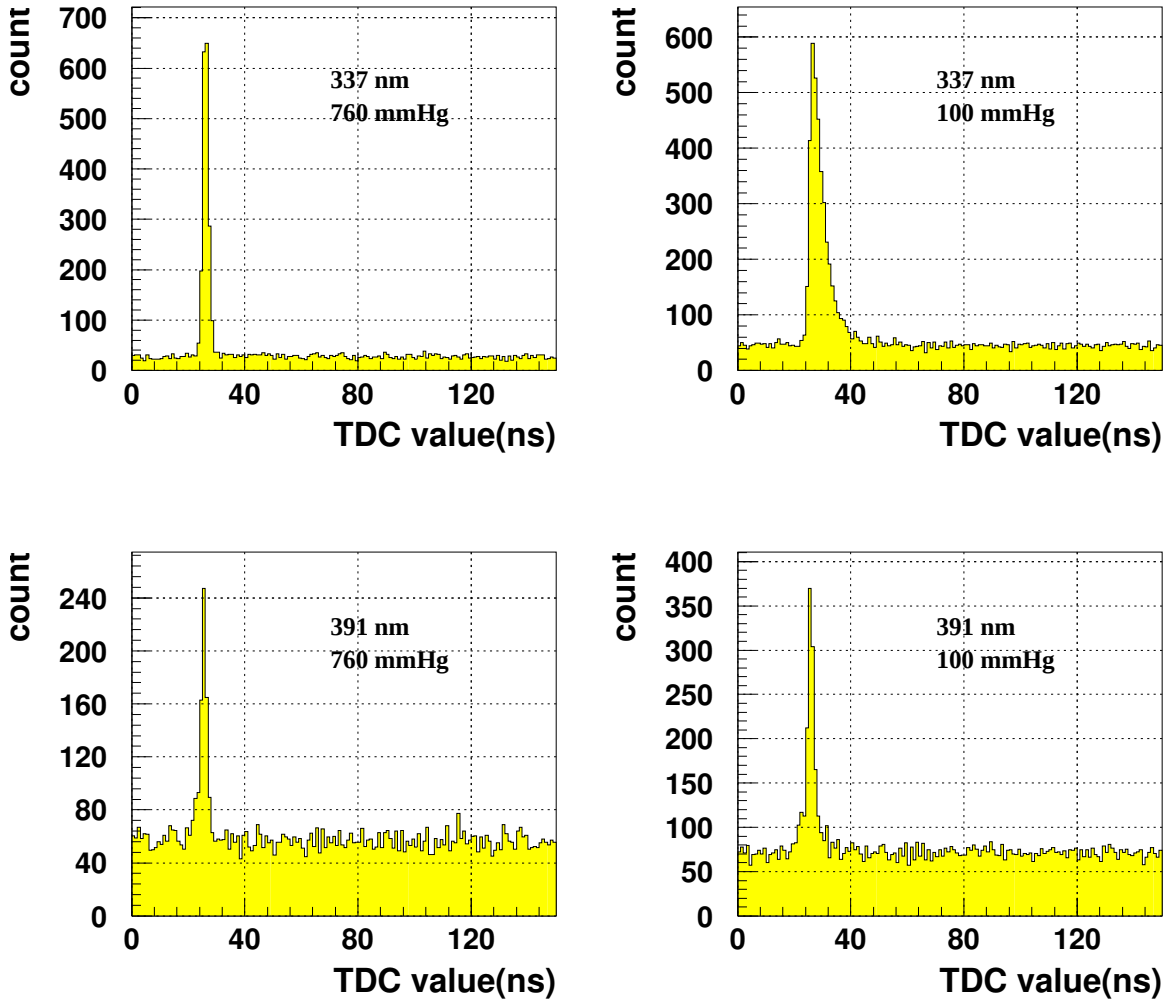


Figure 5: *Four examples of TDC distribution showing relative time between electrons and photons. The cases of pressure of 760 mmHg and 100 mmHg are shown for two narrow band filters, 337 nm and 391 nm. In the case of the 337 nm band, exponential decay is clearly observed at 100 mmHg. In comparison, the decay time for the 391 nm band is much shorter.*

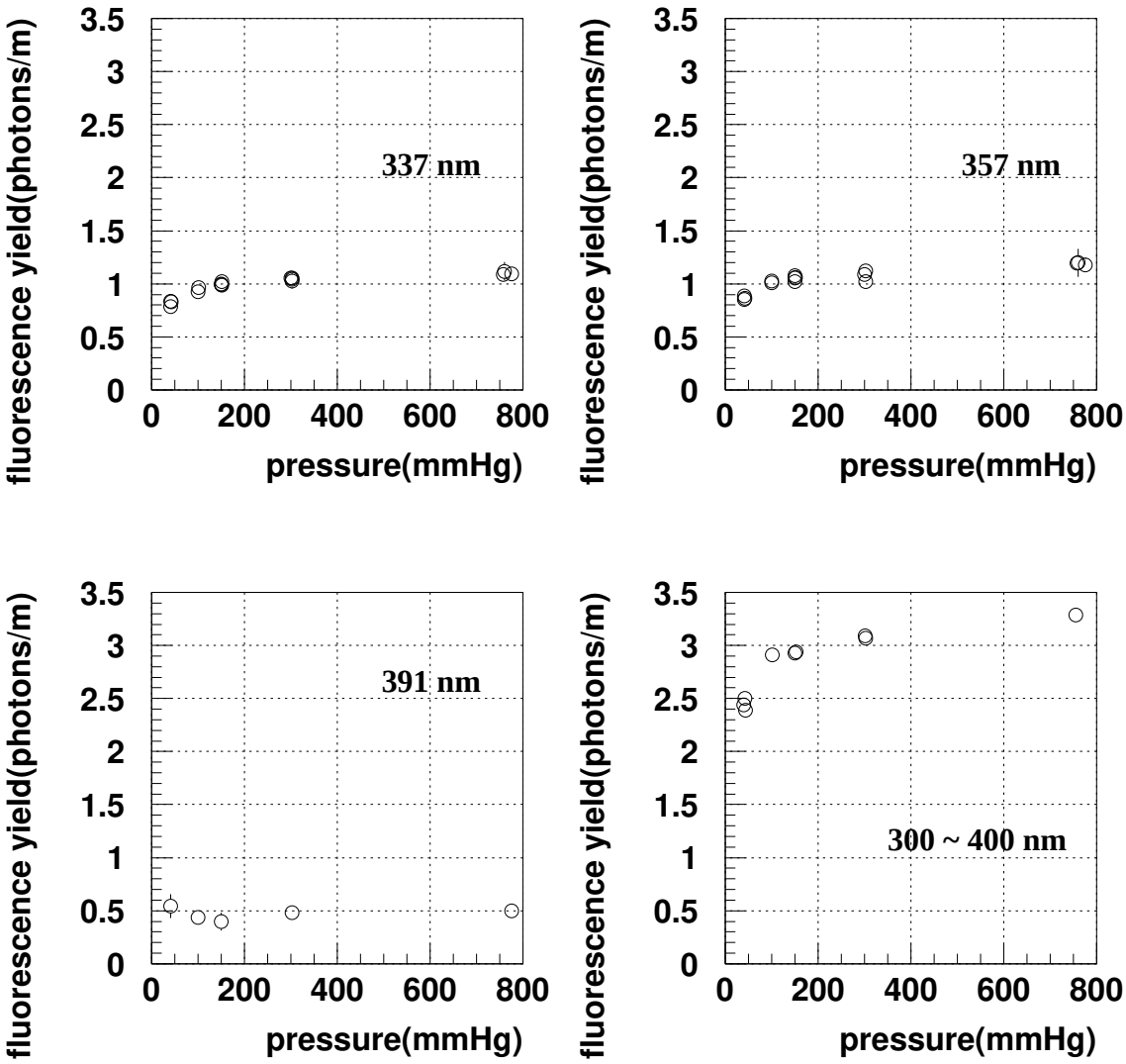


Figure 6: *The pressure dependence of nitrogen fluorescence in dry air at 15° C with 1.4 MeV electrons.*

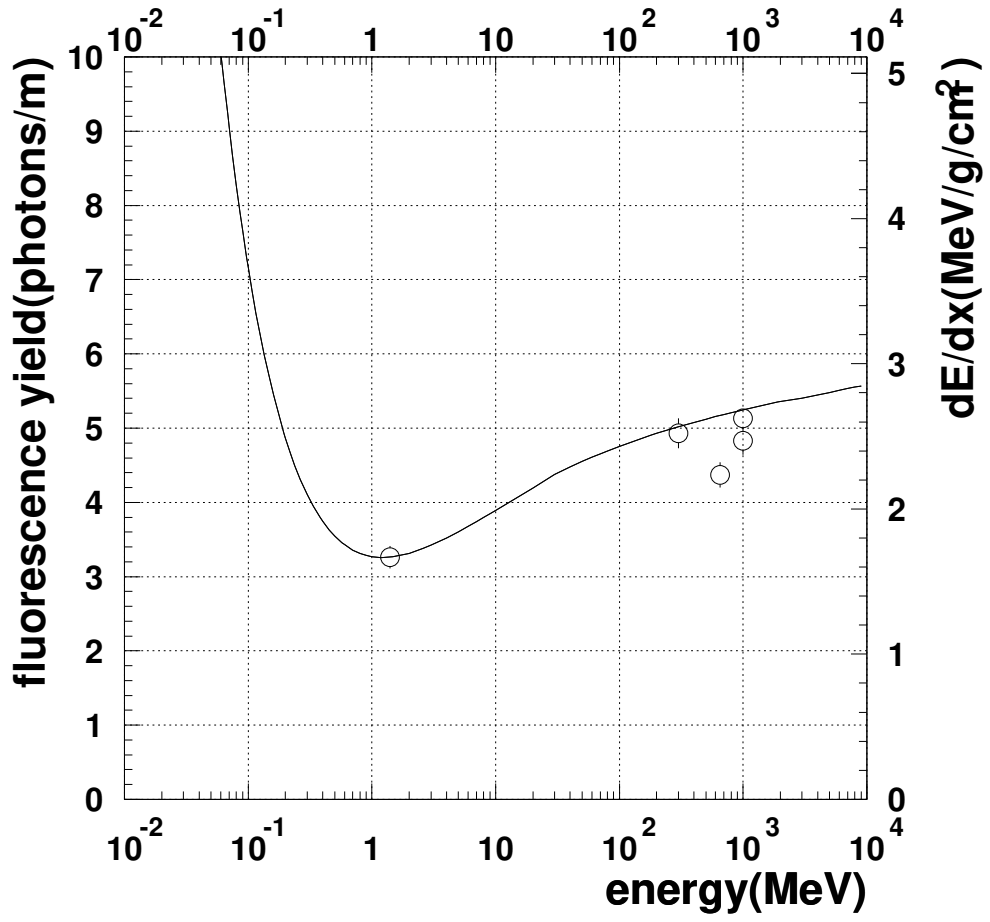


Figure 7: *Energy dependence of nitrogen fluorescence between 300 and 400 nm in dry air at a pressure of 760 mmHg. The* $\frac{dE}{dx}$ *curve is shown as a solid line. The scale of the fluorescence yield is adjusted so that the 1.4 MeV point lies on the* $\frac{dE}{dx}$ *curve.*

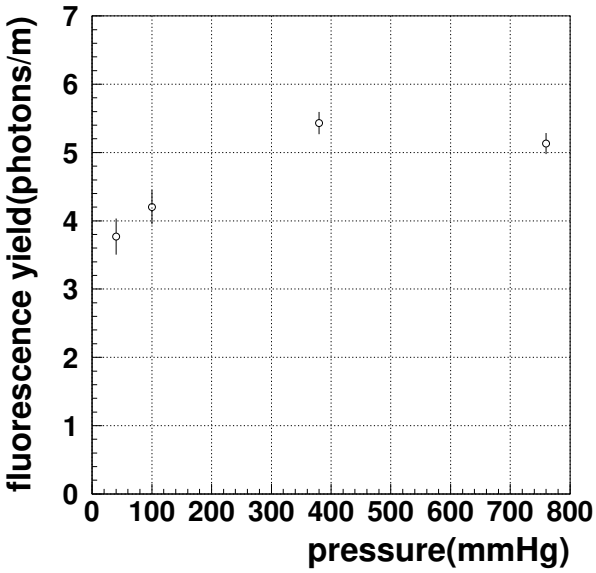


Figure 8: *A typical fluorescence yield between 300 and 400 nm as a function of pressure obtained with 1000 MeV electrons.*

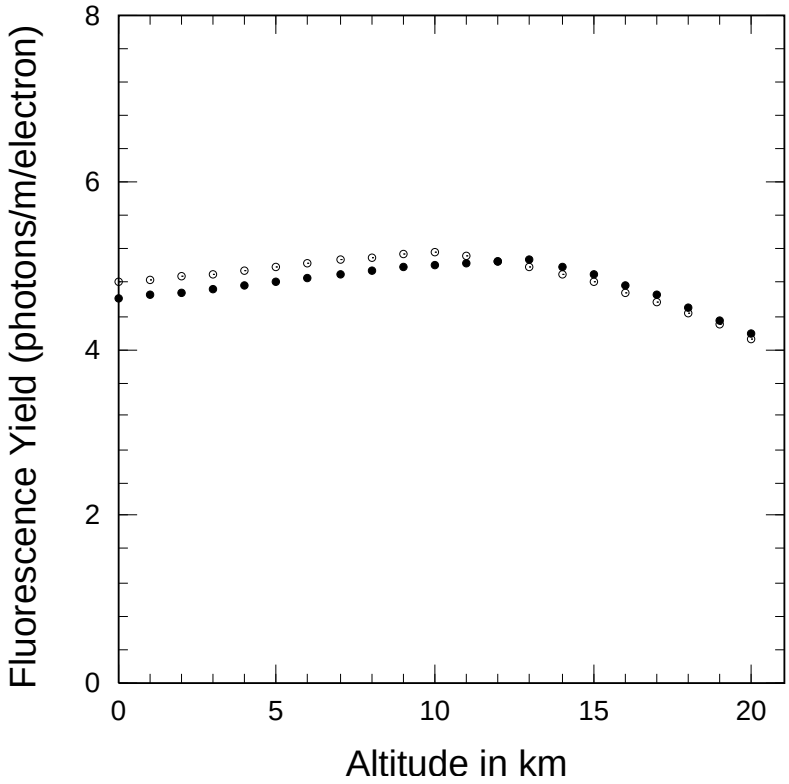


Figure 9: *Fluorescence yield between 300 nm and 400 nm of an 80 MeV electron as a function of altitude. This calculation employed a typical mid-latitude summer atmospheric model with a surface temperature of 296 K (closed circle) and a similar winter model with a surface temperature of 273 K(open circles).*